

## Interference of surface plasmon polaritons excited at hole pairs in thin gold films

V. Häfele, F. de León-Pérez, A. Hohenau, L. Martín-Moreno, H. Plank et al.

Citation: *Appl. Phys. Lett.* **101**, 201102 (2012); doi: 10.1063/1.4767523

View online: <http://dx.doi.org/10.1063/1.4767523>

View Table of Contents: <http://apl.aip.org/resource/1/APPLAB/v101/i20>

Published by the [American Institute of Physics](#).

---

### Additional information on *Appl. Phys. Lett.*

Journal Homepage: <http://apl.aip.org/>

Journal Information: [http://apl.aip.org/about/about\\_the\\_journal](http://apl.aip.org/about/about_the_journal)

Top downloads: [http://apl.aip.org/features/most\\_downloaded](http://apl.aip.org/features/most_downloaded)

Information for Authors: <http://apl.aip.org/authors>

## ADVERTISEMENT



**Goodfellow**  
metals • ceramics • polymers • composites  
70,000 products  
450 different materials  
**small quantities fast**

[www.goodfellowusa.com](http://www.goodfellowusa.com)

## Interference of surface plasmon polaritons excited at hole pairs in thin gold films

V. Häfele,<sup>1</sup> F. de León-Pérez,<sup>2,3</sup> A. Hohenau,<sup>1</sup> L. Martín-Moreno,<sup>2</sup> H. Plank,<sup>4</sup> J. R. Krenn,<sup>1</sup> and A. Leitner<sup>1</sup>

<sup>1</sup>Institute of Physics, Karl-Franzens University Graz, Universitätsplatz 5, 8010 Graz, Austria

<sup>2</sup>Instituto de Ciencia de Materiales de Aragón and Departamento de Física de la Materia Condensada, CSIC-Universidad de Zaragoza, E-50009 Zaragoza, Spain

<sup>3</sup>Centro Universitario de la Defensa de Zaragoza, Ctra. de Huesca s/n, E-50090 Zaragoza, Spain

<sup>4</sup>Institute for Electron Microscopy and Fine Structure Research (FELMI), Graz University of Technology and Graz Center for Electron Microscopy (ZFE), Austrian Cooperative Research (ACR), Steyrergasse 17, A-8010 Graz, Austria

(Received 22 August 2012; accepted 31 October 2012; published online 12 November 2012)

The excitation of surface plasmon polaritons by focusing a laser beam onto a hole pair in a thin gold film is studied both experimentally and theoretically. By means of leakage radiation microscopy we quantitatively measure the light-plasmon coupling efficiency as a function of the hole distance. We find a modulation of the coupling efficiency as a function of hole distance that strongly depends on the polarization direction of the incident light, in agreement with theoretical simulations. © 2012 American Institute of Physics. [<http://dx.doi.org/10.1063/1.4767523>]

The extraordinary optical transmission through subwavelength sized holes in opaque metal films mediated by surface plasmon polaritons (SPPs) has attracted considerable recent interest.<sup>1</sup> The cooperative electrodynamic action of the individual holes corresponding to SPP interference, waveguide effects inside the holes, and light directly transmitted through the holes has been analyzed in both experiment and theory.<sup>2–5</sup> For a thorough understanding it has been proven an efficient strategy to study the properties of simplified systems as, e.g., pairs of holes, and then to deduce the behaviour of more complex systems as hole arrays.<sup>4–11</sup> Pacifici *et al.*<sup>10</sup> have studied hole pairs in 250 nm thick gold films and interpreted the observed variation of the transmitted light intensity as a function of the hole distance by the interplay of direct light transmission and SPP excitation at the holes. An extensive theoretical study of both the transmitted light and SPP intensities in hole pair systems has highlighted a strong dependence of the overall SPP intensity on the hole distance.<sup>12</sup> In this letter, we quantitatively measure the intensities of SPPs launched from subwavelength-sized hole pairs. We find that the SPP intensity varies with hole distance due to SPP interference, a finding in accordance with a theoretical model based on the coupled-mode method.

Circular holes of 250 nm diameter were etched in 80 nm thick gold films on 100  $\mu\text{m}$  thick glass substrate by a focussed beam of Ga ions (30 kV acceleration voltage, 1 pA etching current, dose per hole  $1 \times 10^{-12}$  C). The inset in Fig. 1 shows a scanning electron microscope (SEM) image of a typical hole pair. For detecting the SPPs we apply leakage radiation microscopy (LRM) as described in previous work.<sup>13</sup> In brief, the 800 nm emission of a titanium-sapphire laser is focussed by the microscope objective O1 (Fig. 1) with a numerical aperture of 0.6 onto the air side of the metal film to a minimum focus diameter of about twice the wavelength. To ensure identical illumination power at both holes, the focus is centered at the symmetry point between the holes. As the light intensity at the hole sites decreases with

increasing hole distance we apply a correction function obtained from measuring light-plasmon coupling while scanning a single hole through the focus.

The glass side of the sample is attached by immersion oil to the microscope objective O2 with a numerical aperture (1.25) sufficiently large to accept SPP leakage radiation with an emission angle  $\theta_{LR}$  (with respect to the substrate normal) defined by  $k_{spp} = n \times k_0 \times \sin \theta_{LR}$ , where  $k_{spp}$  and  $k_0$  are the wave numbers of the SPP and light, respectively, and  $n$  is the refractive index of the glass substrate. The back focal plane of O2 is imaged by lenses L1 and L2 in a 4f configuration to the plane of a circular beam blocker that can selectively remove all (scattered) light wavevector components smaller than  $0.83 k_{spp}$ . Lenses L3 and L4 allow to choose either the real space or back focal plane image on the CCD camera.

For the theoretical description of the hole pair system we use the coupled-mode method (CMM),<sup>4</sup> solving Maxwell's equations self-consistently using a convenient representation

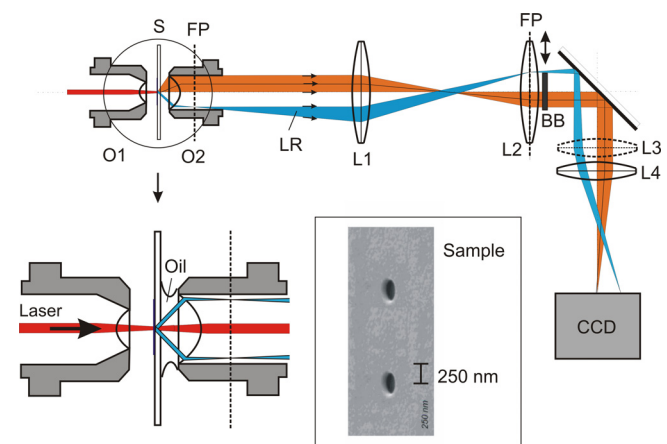


FIG. 1. Optical setup for leakage radiation microscopy. O1 microscope objective for focussing the laser beam, S sample, O2 imaging microscope objective, BFP back focal plane, LR leakage radiation, L1 to L4 auxiliary lenses, BB beam blocker, CCD charge coupled device image sensor. The inset shows a SEM image of a hole pair in an 80 nm thick gold film.

for the electromagnetic fields.<sup>4</sup> In both substrate and superstrate the fields are expanded into an infinite set of plane waves with both polarizations, parallel and normal to the hole pair axis. Inside the holes the natural basis is a set of circular waveguide modes, where convergence is quickly achieved with a small number of such modes.<sup>14</sup> In fact, considering only the fundamental waveguide mode already provides a good approximation for our problem.<sup>12</sup> The parallel components of the fields are matched at the metal/dielectric interface using surface impedance boundary conditions.<sup>14</sup> Although this neglects the tunnelling of electromagnetic energy between the two metal surfaces, this effect is not relevant for a metal thickness larger than a few skin depths. At the lateral walls of the holes we choose the perfect electric conductor (PEC) approximation for the sake of analytical simplicity. We are thus neglecting absorption losses at the walls. Nevertheless, we upgrade the PEC approximation introducing two phenomenological corrections. First, the propagation constant of the PEC fundamental mode is replaced by the one computed for a real metal. This improves the comparison between CMM and both experimental and finite difference time domain (FDTD) results (not shown here) for both the spectral position of the peaks and the dependence of optical properties on the metal thickness. Second, enlarging the radius of the hole by one skin depth simulates the real penetration of in field into the metallic walls. This value for the enlargement was again found to provide the best agreement with FDTD simulations for an infinite periodic array of holes.<sup>15</sup> After matching the fields at the interface we arrive at a system of tight binding-like equations for the amplitude of the fundamental waveguide mode at the hole-openings, which can be solved analytically for a hole-pair.<sup>12</sup> The flux power traversing the hole is distributed into two channels: (i) out-of-plane radiation, freely propagating into the far-field, and (ii) SPP power, scattered along the metal plane. The calculation of these two quantities is straightforward within the CMM after we know the amplitude of the fundamental waveguide mode at the hole openings. Only the SPP scattered power is considered hereafter. Reference 12 shows that given the value of amplitude at the input side of the hole,  $E$ , the interference pattern of the in-plane scattering power is determined by the SPP optical path between the two holes,  $k_{spp} R$ , where  $R$  is the distance between the hole centres. In contrast to the far field radiation, the normalized SPP intensity depends weakly on the hole size.<sup>12</sup>

While the formulae derived in Ref. 12 apply to free-standing metal films the case considered here includes a sub-

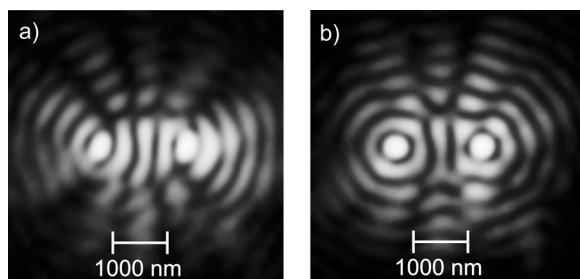


FIG. 2. LRM images of a hole pair aligned along the horizontal direction in a 80 nm thick gold film. The centre-to-centre hole distance is 1600 nm. The polarization direction of the incident laser beam is (a) parallel and (b) normal to the pair axis.

strate. However, the general physical trends are expected to be the same.

Fig. 2 shows real space LRM images of a hole pair with 1600 nm hole distance. We observe a distinct intensity pattern due to SPP interference that depends strongly on the polarization direction of the exciting light. Contrary to the case of light-plasmon coupling mediated by nanoparticles on a thin film,<sup>16</sup> holes give rise to a significant amount of transmitted scattered light, leading to a rather uniform background intensity within the acceptance angle of the microscope objective. As the circular beam blocker can only suppresses this background within an angle range smaller than  $\theta_{LR}$ , light scattered to higher angles contributes to the SPP images in Fig. 2, hindering the detailed analysis of the SPP intensities. Therefore we turn to the analysis of the back focal plane images which provides the possibility to separate the SPP related leakage light from the scattering contributions.

A set of back focal plane images is shown in Fig. 3. As a reference, panels (a) and (b) depict images of single holes

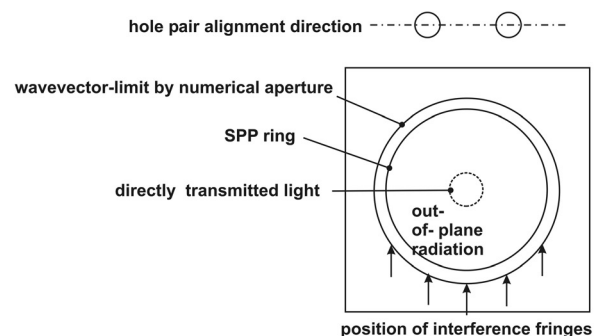
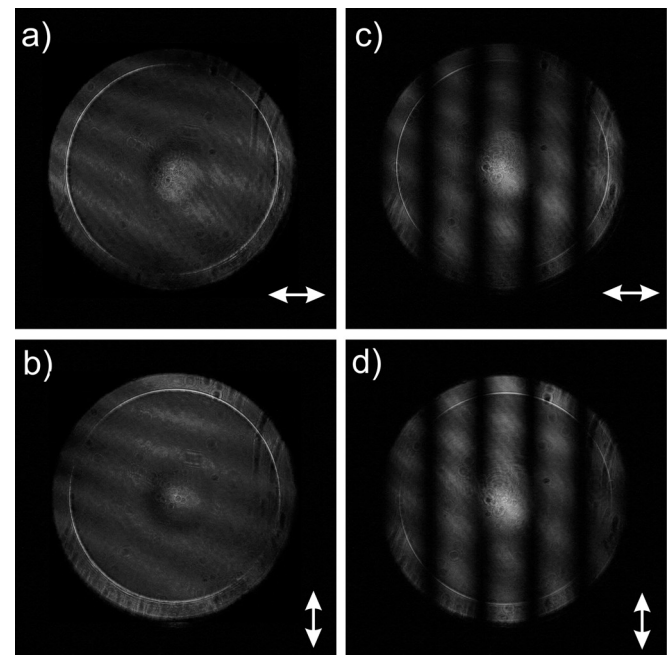


FIG. 3. Back focal plane images of a single hole for (a) horizontal and (b) vertical polarization direction. (c), (d) The corresponding images for a horizontally aligned hole pair. Polarization directions are indicated by double-sided arrows. All holes measure 250 nm in diameter, the hole distance is 1600 nm. Image contrast is optimized for best visibility of the interference pattern. The inset at the bottom highlights the respective features in the images. SPP-ring bright circular zone caused by leakage radiation.

for horizontal and vertical polarization of the exciting laser light, respectively. Panels (c) and (d) show the corresponding images for hole pairs with 1600 nm hole distance. In the images the distance of an image point from the image centre corresponds to the wavevector component parallel to the sample plane. The bright narrow ring segments represent the SPP leakage radiation defined by  $k_{SPP}$ , the background intensity is due to transmitted light scattered by the holes, as discussed above, and the weak central spot is due to light directly transmitted through the gold film. The latter feature remains visible when imaging a gold film area without any hole. The outer circular limit of the bright area is determined by the finite numerical aperture (1.25) of the objective. Importantly, the central circular beam block has been removed for these images as it is obsolete due to the data processing as discussed below.

As expected from a local SPP source we find an angular dependence of the SPP leakage following a  $\cos^2 \theta$  dependence ( $\theta$  being the azimuthal angle with respect to the polarization direction), in contrast to a  $\sin^2 \theta$  dependence of a dipole radiating to the far field. For the hole pair the interference between both coherent SPP sources leads to significant vertical interference fringes (Figs. 3(c) and 3(d)) due to momentum transfer parallel to the hole pair axis. As these fringes shift over the SPP ring as a function of hole distance, the overall SPP intensity is modulated. We note that first, the weak almost horizontal fringes in Figs. 3(a) and 3(b) are due to an etaloning effect of the camera which is of no principal importance but represents a noise source limiting measurement accuracy. Second, due to some polarization misalign-

ment the laser polarization deviates about  $10^\circ$  from the vertical and horizontal directions which however does not significantly influence our conclusions drawn below.

For the quantitative evaluation of the leakage radiation data we processed the images numerically by selectively summing up the intensities of all image pixels corresponding to the SPP specific wavevector components. Fig. 4(a) shows the thereby retrieved power data as a function of the centre-to-centre distance of the holes (normalized to the SPP wavelength  $\lambda_{spp} = 784$  nm) for the horizontal polarization direction. The SPP power is normalized to the twofold of the power measured from a single hole for otherwise identical parameters. We find a clear periodicity described by  $\lambda_{spp}$  that agrees well with the CMM based theoretical calculation plotted by the solid line. In simple physical terms, due to the SPP emission patterns from the single holes intensity maxima occur close to the conditions for constructive SPP interference,  $R = m\lambda_{spp}$  ( $m = 1, 2, 3, \dots$ ), while minima appear close to  $R = (2m - 1)\lambda_{spp}/2$ .<sup>13</sup> It should be noted that the normalized SPP power rises still to 1.6 at  $R/\lambda_{spp} = 1$  though the SPP decay depends linearly on  $R$ .

The uncertainty of our data points is mainly given by the above mentioned camera effects and are estimated to  $\pm 0.15$  in Fig. 4. At short hole distances where near field interaction and non-SPP surface modes are expected to contribute significant deviations from the SPP power characteristics reported here are expected<sup>17,18</sup> which is however beyond the scope of this study.

For the polarization direction normal to the pair axis we expect a much weaker dependence of the SPP power on hole distance. This becomes clear from Fig. 3(d), where a shift of the interference fringes as a function of  $R$  has clearly less influence on the overall SPP intensity than for the case of horizontal polarization depicted in Fig. 3(c). This is well corroborated by the simulation result, plotted as the solid curve in Fig. 4(b). Indeed, our experimental data show the same trend, however at a rather poor signal-to-noise ratio.

Finally, we compare our results with previous reports on the light intensity transmitted through a hole pair, i.e., out-of-plane radiation.<sup>9,10</sup> This radiation channel is complementary to the in-plane radiation (SPP) channel studied here as the energy traversing the holes is distributed into both channels.<sup>12</sup> Reference 10 shows that the out-of-plane normalized intensity has maxima at  $(m-1/4)\lambda_{spp}$ , while the normalized intensity is equal to 1 when the condition for constructive interference of SPPs ( $R = m\lambda_{spp}$ ) is fulfilled. Similar trends are found in our case (not shown). Pacifici *et al.*<sup>10</sup> stressed that there is neither a transmission enhancement nor suppression of the normalized far-field intensity at  $R = m\lambda_{spp}$  though their experimental results have been nicely fitted to a SPP interference model. Our results shed light on such a counterintuitive behaviour: A transmission enhancement at  $R = m\lambda_{spp}$  is obtained only for the energy scattered into SPPs along the metal plane. As the fraction of the incident light radiated to the far field behaves as a complementary channel to the light scattered along the metal plane, the interference conditions for the two channels are fulfilled for different values of  $R$ .

In summary, we have measured the light-SPP coupling efficiency of a subwavelength hole pair in a gold film as a function of the hole distance. The SPP intensity shows an

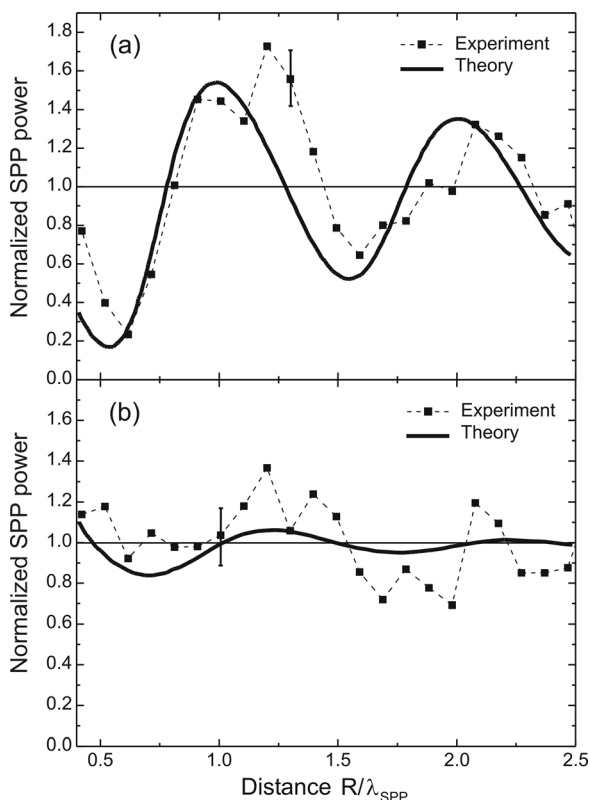


FIG. 4. Measured normalized SPP power vs. normalized hole distance for polarization directions of the incident light (a) parallel to the pair axis and (b) normal to the pair axis (symbols). The full lines show the theoretical calculations.

interference pattern modulated by the SPP wavelength and strongly depending on the polarization direction of the incident light. Extreme values for in-plane SPP intensity fulfil the conditions of interference of SPPs at the metal/air interface, in contrast to previous reports of the normalized out-of-plane intensity, which is equal to 1 for  $R = m\lambda_{spp}$ .

The authors gratefully acknowledge financial support from EC project Acción Integrada Ref. AT2009-0027 and ES12/2010 and Spanish MECD under Contract No. MAT2011-28581-C02. F.d.L.P. and L.M.M. acknowledge helpful discussions with A. Yu. Nikitin.

- <sup>1</sup>T. W. Ebbesen, H. J. Lezec, H. F. Ghaemi, T. Thio, and P. A. Wolff, *Nature (London)* **391**, 667 (1998).  
<sup>2</sup>L. Martín-Moreno, F. J. García-Vidal, H. J. Lezec, K. M. Pellerin, T. Thio, J. B. Pendry, and T. W. Ebbesen, *Phys. Rev. Lett.* **86**, 1114 (2001).  
<sup>3</sup>C. Genet and T. W. Ebbesen, *Nature (London)* **445**, 39 (2007).  
<sup>4</sup>F. J. García-Vidal, L. Martín-Moreno, T. W. Ebbesen, and L. Kuipers, *Rev. Mod. Phys.* **82**, 729 (2010).  
<sup>5</sup>P. Johansson, *Phys. Rev. B* **83**, 195408 (2011).  
<sup>6</sup>C. Sönnichsen, A. C. Duch, G. Steininger, M. Koch, G. von Plessen, and J. Feldmann, *Appl. Phys. Lett.* **76**, 140 (2000).

- <sup>7</sup>H. F. Schouten, N. Kuzmin, G. Dubois, T. D. Visser, G. Gbur, P. F. A. Alkemade, H. Blok, G. W. t Hooft, D. Lenstra, and E. R. Eliel, *Phys. Rev. Lett.* **94**, 053901 (2005).  
<sup>8</sup>P. Lalanne, J. P. Hugonin, and J. C. Rodier, *Phys. Rev. Lett.* **95**, 263902 (2005).  
<sup>9</sup>Y. Alaverdyan, B. Sepulveda, L. Eurenus, E. Olsson, and M. Käll, *Nat. Phys.* **3**, 884 (2007).  
<sup>10</sup>D. Pacifici, H. J. Lezec, L. A. Sweatlock, R. J. Walters, and H. A. Atwater, *Opt. Express* **16**, 9222 (2008).  
<sup>11</sup>J. Alegret, P. Johansson, and M. Käll, *New J. Phys.* **10**, 105004 (2008).  
<sup>12</sup>F. de León-Pérez, F. J. García-Vidal, and L. Martín-Moreno, *Phys. Rev. B* **84**, 125414 (2011).  
<sup>13</sup>A.-L. Baudrion, F. de Leon-Perez, O. Mahboub, A. Hohenau, H. Ditlbacher, F. J. Garcia-Vidal, J. Dintinger, T. W. Ebbesen, L. Martín-Moreno, and J. R. Krenn, *Opt. Express* **16**, 3420 (2008).  
<sup>14</sup>F. de León-Pérez, G. Brucoli, F. J. García-Vidal, and L. Martín-Moreno, *New J. Phys.* **10**, 105017 (2008).  
<sup>15</sup>F. Przybilla, A. Degiron, C. Genet, T. W. Ebbesen, F. de León-Pérez, J. Bravo-Abad, J. F. J. García-Vidal, and L. Martín-Moreno, *Opt. Express* **16**, 9571 (2008).  
<sup>16</sup>A. Drezet, A. Hohenau, A. L. Stepanov, H. Ditlbacher, B. Steinberger, N. Galler, F. R. Aussenegg, A. Leitner, and J. R. Krenn, *Appl. Phys. Lett.* **89**, 091117 (2006).  
<sup>17</sup>A. Yu. Nikitin, F. J. García-Vidal, and L. Martín-Moreno, *Phys. Rev. Lett.* **105**, 073902 (2010).  
<sup>18</sup>H. Liu and P. Lalanne, *Nature (London)* **452**, 728 (2008).